Electronic structure and spectroscopic properties of thulium monochalcogenides

S. Lebègue,[1] G. Santi,[2] A. Svane,[2] O. Bengone,[3] M. I. Katsnelson,[4] A. I. Lichtenstein,[5] and O. Eriksson[1]
[1]*Department of Physics, University of Uppsala, SE-75121 Uppsala, Sweden*
[2]*Department of Physics and Astronomy, University of Aarhus, DK-8000 Aarhus C, Denmark*
[3]*Institut de Physique et de Chimie des Matériaux de Strasbourg (IPCMS), UMR 7504 CNRS-ULP, 23 rue du Loess, 67034 Strasbourg, France*
[4]*Institute for Molecules and Materials, Radboud University Nijmegen, NL-6525 ED Nijmegen, The Netherlands*
[5]*Institute of Theoretical Physics, University of Hamburg, 20355 Hamburg, Germany*
(Received 12 August 2005; published 2 December 2005)

The electronic structure of the thulium monochalcogenides TmS, TmSe, and TmTe is studied with several theoretical approaches. The total energy is evaluated with the self-interaction corrected local-spin density approximation, whereby the Tm ions are described with either twelve or thirteen localized *f* electrons with the remaining electrons forming bands. The comparisons of these two scenarios reveal the valency shift of the Tm ion through the series. The spectral functions of Tm*X* compounds are calculated including multiplet effects, and they are compared to experimental x-ray photoemission spectra. The basic tool is the Hubbard-I approximation in which the embedding of an isolated f^n ion in a solid is performed by modifying the crystal Hamiltonian as obtained from the local-density approximation with the atomic self-energy of the ion. The parameters of the model are obtained from the self-consistent band structure calculation. The agreement with experiment is excellent, reproducing all significant multiplet structures.

DOI: 10.1103/PhysRevB.72.245102 PACS number(s): 71.28.+d, 71.20.Eh, 71.15.Nc, 79.60.−i

I. INTRODUCTION

The Tm monochalcogenides have attracted a lot of interest due to their complex physical and chemical properties.[1] At ambient pressures TmS is a trivalent metal,[2] TmSe is in a mixed valence state[2–4] (with a valency between 2.55 and 2.72), and TmTe is a divalent, magnetic semiconductor.[2] The resistivity of TmSe shows a Kondo-like logarithmic temperature dependence at high temperatures, whereas at low temperatures TmSe is suggested to be insulating.[5] The resistivity of TmS is also complex, with a Kondo-like behavior.[6] High pressure experiments[7] show that TmTe is divalent and insulating up to a pressure of 2 GPa, a mixed valent between 2 and 6 GPa, and a trivalent metal above 6 GPa. In addition a crystallographic phase transition has been reported at ~8 GPa, from the NaCl structure to a tetragonal phase.[8–10] The optical properties of $TmSe_{1-x}Te_x$ alloys have also been measured,[11] in particular the Kerr rotation spectrum.

The low temperature properties of TmTe have been studied with particular emphasis on the quadrupolar ordering that occurs due to the crystal field split Γ_8 state.[12] By measurements of susceptibility, elastic constants, magnetization, and specific heat it was concluded that quadrupolar ordering occurred below 1.7 K.[12] Neutron scattering experiments[13,14] were consistent with this conclusion.

The phonons were measured in TmTe by using far infrared spectroscopy and Raman scattering,[15] and these measurements agreed well with the theoretical phonon distribution curve calculated by Jha.[16] Concerning the electronic structure, first principles calculations have been carried out for the Tm chalcogenides[17–19] both in the local spin density approximation (LSDA) and local density approximation (LDA)+U. However, the only conclusion that can be drawn from the comparison with photoemission spectra is that neither of these approximations can reproduce the features in the observed data due to their lack of atomic multiplet effects.

In the present paper we aim at improving the agreement between theory and experiment and in order to do this we adopt the approach of Ref. 20 to calculate the spectroscopic data of the Tm-chalcogenides. The main advantage with this approach is that atomic multiplet effects naturally enter the one-particle Green's function and hence it is appropriate for localized electron systems, such as the 4*f* states in the Tm chalcogenides. The spectroscopic data were measured in Refs. 21–23 and a detailed comparison between theory and experiment at ambient conditions is made here.

In addition to addressing the spectroscopical properties theoretically we present here also an analysis of the cohesive properties and in particular pressure induced phase transitions, by means of a self-interaction corrected local-spin density functional. The rest of this paper is organized as follows: In Sec. II we present our theoretical methods, Sec. III contains our results, and in Sec. IV we summarize and offer our conclusions.

II. THEORY

A. The SIC-LSD total-energy method

The self-interaction correction to the local-spin density approximation (SIC-LSD) formalism that is used here to treat the localized *f* states has been described in details elsewhere,[24–26] but we shall review here the key concepts.

In density functional theory (DFT),[27–29] the ground state of a spin-polarized system is obtained by minimizing the spin density functional of the energy,

$$E[n,m] = T[n,m] + U[n] + V_{\mathrm{ext}}[n] + E_{\mathrm{xc}}[n,m], \qquad (1)$$

with $n(\mathbf{r})=n_\uparrow(\mathbf{r})+n_\downarrow(\mathbf{r})$ and $m(\mathbf{r})=n_\uparrow(\mathbf{r})-n_\downarrow(\mathbf{r})$ being the total and magnetization densities, respectively. T, U, V_{ext}, and E_{xc} are the kinetic energy, the Hartree energy, the energy of

the external potential, and the exchange-correlation energy. The most used and probably most successful approximation to the exchange-correlation functional is the LSDA in which

$$E_{\mathrm{xc}}^{\mathrm{LSDA}}[n,m] = \int d^3\mathbf{r}\,\epsilon_{\mathrm{xc}}^{\mathrm{hom}}[n(\mathbf{r}),m(\mathbf{r})]n(\mathbf{r}), \tag{2}$$

where $\epsilon_{\mathrm{xc}}^{\mathrm{hom}}(n,m)$ is the exchange-correlation energy of the homogeneous electron gas of density n and magnetization density m. The correct form of the exchange-correlation functional has the property for any single-particle densities n_α and $m_\alpha = n_\alpha$ as it exactly cancels out the Coulomb self-interaction,[30] i.e., $E_{\mathrm{xc}}[n_\alpha,n_\alpha]+U[n_\alpha]=0$. This is, however, not true in the LSDA for localized states (it still holds for delocalized Bloch states, where both terms vanish in the thermodynamic limit). Hence, the LSDA contains a spurious self-interaction

$$\delta_\alpha = U[n_\alpha] + E_{\mathrm{xc}}^{\mathrm{LSDA}}[n_\alpha,n_\alpha]. \tag{3}$$

The SIC-LSD approximation consists of subtracting this term from the energy functional for each localized orbital, which results, after minimization, in an orbital-dependent Kohn-Sham equation,[24,25]

$$(H_0 + V_\alpha^{\mathrm{SIC}})|\psi_\alpha\rangle = \sum_{\alpha'} \lambda_{\alpha,\alpha'}|\psi_{\alpha'}\rangle, \tag{4}$$

$$H_0 = -\boldsymbol{\nabla}^2 + V_H(\mathbf{r}) + V_{\mathrm{ext}}(\mathbf{r}) + V_{\mathrm{xc}}^{\mathrm{LSDA}}(n(\mathbf{r}),m(\mathbf{r})), \tag{5}$$

$$V_\alpha^{\mathrm{SIC}}(\mathbf{r}) = -2\int d\mathbf{r}'\left(\frac{n_\alpha(\mathbf{r}')}{|\mathbf{r}-\mathbf{r}'|} - V_{\mathrm{xc}}^{\mathrm{LSDA}}(n_\alpha(\mathbf{r}),n_\alpha(\mathbf{r}))\right), \tag{6}$$

where V_H, V_{ext}, and $V_{\mathrm{xc}}^{\mathrm{LSDA}}$ are the Hartree, external, and LSDA exchange-correlation potentials. In Eq. (4), the $\lambda_{\alpha,\alpha'}$ are the Lagrange multipliers associated to the orthonormality constraint between the $|\psi_\alpha\rangle$. As we have already mentioned, $V_\alpha^{\mathrm{SIC}}(\mathbf{r})$ vanishes identically for an extended Bloch state and the LSDA "ground" state is therefore a suitable solution of Eq. (4), i.e., it makes the SIC energy functional stationary. In our implementation, Eq. (4) is solved by steepest descent and unitary state mixing in order to find the lowest energy state corresponding to a predefined number of localized electrons.[24,25]

B. Spectral functions within the Hubbard-I approximation

For systems showing strong correlations (i.e., the Coulomb interaction exceeds the band width, $U/W>1$) as is the case for rare earth compounds, calculations based on the DFT are often unable to reproduce experimental data. This is especially true for spectroscopic data and arises from the fact that atomic multiplets are present in the spectrum that cannot be described by one-particle approaches such as the DFT. To achieve a satisfactory description of this kind of phenomenon, one has to use a theory which combines the many body effects due to localization of electrons, with the bands from delocalized states. One way to do that is to use the so-called Hubbard-I approximation (HIA).[31] This method is described shortly here, a full account may be found in Ref. 20. A simple diagrammatic derivation of this approximation is given in the Appendix. First, the eigenvalues E_γ and eigenvectors $|\gamma\rangle$ of a Hubbard Hamiltonian representing an atomic f^n shell and written as

$$H^{at} = \frac{1}{2}\sum_{\{m_j\}} U_{m_1m_2m_3m_4}c_{m_1}^+c_{m_2}^+c_{m_3}c_{m_4} + \xi\sum_i \vec{l}_i\cdot\vec{s}_i - \mu\sum_m c_m^+c_m, \tag{7}$$

are obtained by exact diagonalization. Here, indices m_j refer to the individual orbitals of the f^n shell including spin, i.e., $m_j=1,\ldots,14$, for f orbitals. The spin-orbit coupling is included in the second term where ξ is the spin-orbit constant related to the derivative of the radial potential and $\vec{l}_i$ and $\vec{s}_i$ are the orbital moment and spin operators for the ith electron in that shell. The chemical potential, μ, included in the third term, is treated here as an adjustable parameter. The four-center integrals of the Coulomb operator read,

$$U_{m_1m_2m_3m_4} = \sum_{\ell=0}^{\infty}\frac{4\pi}{2\ell+1}\times\sum_{m=-\ell}^{+\ell}\langle m_1|Y_{\ell m}|m_4\rangle\langle m_2|Y_{\ell m}^*|m_3\rangle F^\ell \tag{8}$$

where $\langle m_i|Y_{\ell m}|m_j\rangle$ are the Gaunt coefficients and F^ℓ the Slater integrals. Because of the properties of the Gaunt coefficients, only F^0, F^2, F^4, and F^6 are relevant in the case of f electrons.

The atomic Green's function $G_{mm'}^{at}$ and atomic self-energy, $\Sigma_{mm'}^{at}$, are computed from the eigenvectors of H^{at} as

$$G_{mm'}^{at}(\omega) = \frac{1}{Z}\sum_{\gamma\delta}\frac{\langle\gamma|c_m|\delta\rangle\langle\delta|c_{m'}^+|\gamma\rangle}{\omega+E_\gamma-E_\delta}(e^{-\beta E_\gamma}+e^{-\beta E_\delta}),$$

$$\Sigma_{mm'}^{at}(\omega) = \omega\delta_{mm'} - (G^{at})_{mm'}^{-1}(\omega), \tag{9}$$

where $\beta=1/T$ and Z is the partition function written as $Z=\Sigma_\gamma e^{-\beta E_\gamma}$. Finally, the crystal Green's function $G_{\mathbf{k}}$ is obtained by combining $\Sigma_{mm'}^{at}$ with the Hamiltonian $H_{\mathbf{k}}^{\mathrm{LDA}}$ from a DFT calculation (in our case in the LDA)

$$G_{\mathbf{k}}^{-1}(\omega) = \omega - \Sigma^{at}(\omega) - H_{\mathbf{k}}^{\mathrm{LDA}}. \tag{10}$$

The spectral function $A(\omega)$ is obtained from the Green's function by

$$A(\omega) = \frac{1}{\pi}\,\mathrm{Im}\sum_{\mathbf{k}} G_{\mathbf{k}}(\omega). \tag{11}$$

This is the quantity we will compare to experimental photoemission spectra of TmX compounds, an approximation which ignores the dependence of the photoemission spectrum on the photoelectron matrix elements. The values of the parameters F^ℓ and ξ are determined in an *ab initio* way by using the f partial waves of the self-consistent LDA calculation. However, the first Slater integral, $F^0\equiv U$, needs to be reduced from its bare value in order to get satisfactory agreement with the experiments. This is a well-known effect in all solid state spectroscopies, caused by the screening of the atomiclike electrons by the fast conduction electrons of the

TABLE I. Calculated and experimental lattice constants (from Ref. 37 except where noted) for the different Tm monochalcogenides and for different localization scenarios (f^0, LDA, i.e., "all delocalized;" f^{12}: 12 localized f electrons; f^{13}, 13 localized f electrons).

	Lattice constants (Å)			
TmX compound	Calculated f^0 (LDA)	f^{12}	f^{13}	Experimental
TmS	5.411	5.483	5.757	5.41
TmSe	5.651	5.696	5.990	5.706
TmTe	6.027	6.069	6.363	6.364, 6.049[a]
TmPo	6.228	6.256	6.561	6.256[b]

[a]From Ref. 36.
[b]From Ref. 35.

solid. The only parameter which needs to be adjusted is the chemical potential of the reference atom, which determines the ground state configuration f^n. This chemical potential is crucial for embedding the atom into the solid host in that it relates the atomic energy levels to the solid's energy bands.

Compared to other methods currently used to compute spectra of strongly correlated systems, the present approach lies in between LDA+U (Ref. 32) and dynamical mean-field theory (DMFT) (Refs. 20 and 33) techniques. For the description of spectroscopic properties, the HIA is superior to the LDA+U method or the charge transfer multiplet model,[34] but it cannot improve over the LDA for quantities such as a lattice parameter, a magnetic moment, etc., since it has not yet developed into a (self-consistent) total energy method. Indeed, it can describe multiplet effects contrary to the LDA+U technique where the localized states are accounted for by only a mean-field Hubbard term which is added to the LDA Hamiltonian. Moreover, it can reproduce the **k** dependence of the spectrum [Eq. (10)], which is required for comparison with angle-resolved experiments, in contrast to the charge transfer multiplet model[34] which in addition relies on a large number of parameters (charge transfer energy, hopping strength, crystal field parameters, etc.) to embed the atom into the solid.

III. RESULTS AND DISCUSSION

A. Cohesive properties and pressure-induced valence transitions

The calculated cohesive properties of thulium chalcogenides are summarized in Tables I and II as well as in Fig. 1. Table I compares the calculated equilibrium lattice constants to experimental values. Three scenarios are considered, the LSDA where all f electrons are treated as band states, and the cases of 12 or 13 localized f electrons. The best agreement between the calculated lattice constant and experiment is seen for the LSDA calculation for TmS, for the f^{12} configuration in TmSe and for the f^{13} configuration in TmTe, reflecting the increasing tendency to localization with a larger ligand. However, the fact that the calculated lattice constant in the LSDA are close to the experimental value for TmS (Table I) can only be considered accidental. The experimental lattice constant reported[35] for TmPo breaks this trend, being in fact smaller than that of TmTe. Note, however, that the sample investigated was not stoichiometric and may then

TABLE II. Total energies, E_{tot}, with respect to the f^{12} state, calculated and experimental bulk moduli, B and B_{exp}, as well as calculated transition pressures from f^{12} to f^{13} configurations, P_c and P_c' for the different Tm monochalcogenides and the different localization scenarios [f^0 or LSDA, f^{12} or mixed valent (MV) and f^{13} or divalent]. The transition pressure P_c' is obtained after having shifted down the energy of the f^{12} configuration by 13.5 mRy (see discussion in text). The total energies for the LSDA calculations are not shown (they lie some 1.2 Ry above the other ones) as they are not relevant to our discussion.

		E_{tot} (mRy)	B (GPa)	B_{exp} (GPa)	P_c (GPa)	P_c' (GPa)
TmS	f^0 (LSDA)		78			
	f^{12} (MV)	0.0	87	81[a]	0.5	−3.8
	f^{13} (Tm^{2+})	−1.2	59			
TmSe	f^0 (LSDA)		65			
	f^{12} (MV)	0.0	80	25,[b] 39[c]	4.6	0
	f^{13} (Tm^{2+})	−13.5	48			
TmTe	f^0 (LSDA)		65			
	f^{12} (MV)	0.0	51	30,[d] 45,[e] 83[f]	7.9	3.0
	f^{13} (Tm^{2+})	−24.3	41			
TmPo	f^0 (LSDA)		49			
	f^{12} (MV)	0.0	69	22.2	8.0	
	f^{13} (Tm^{2+})	−37.4	32			

[a]Reference 40.
[b]Reference 41.
[c]Reference 42.
[d]Reference 8.
[e]Reference 9, 43, and 44.
[f]Reference 45.

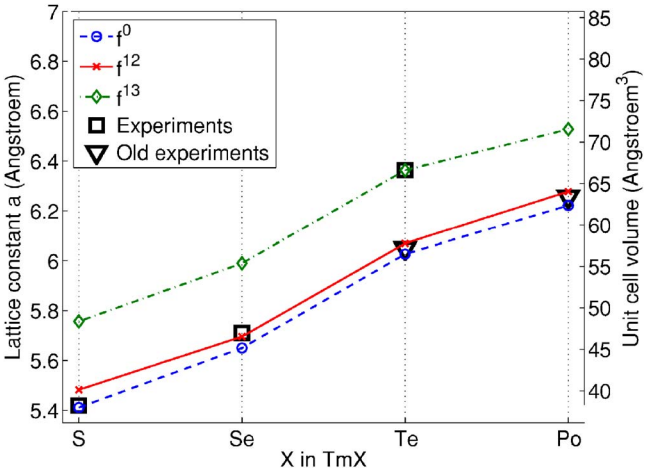

FIG. 1. (Color online) Calculated and experimental lattice constants for the different Tm compounds and for different localization scenarios (see also Table I and text).

be trivalent as a consequence hereof. Similarly, older measurements[36] on TmTe have revealed much lower lattice constants than generally accepted nowadays, probably for the same reason.

In the LSDA calculation an average f occupation between 12 and 13 is found for all compounds. When 12 f electrons are localized, essentially 12 of the occupied LSDA f bands are repopulated as localized states, which does not lead to any significant change in the electron charge distribution and thus affects only slightly the calculated equilibrium lattice constants (Fig. 1). In contrast, when 13 f electrons are taken as localized a significant charge transfer is imposed on the system, the cost of which is balanced by the localization energy gained. The f^{12} calculation leads to an electronic structure characterized by a narrow f band straddling the Fermi level in addition to the 12 localized f electrons. This is similar to the situation found in the Sm chalcogenides in their high pressure intermediate valence phases, which were all well described with the same SIC-LSD method as used here,[38] assuming a localized f^5 (i.e., trivalent) Sm configuration. This scenario is interpreted as the most suitable DFT representation of the intermediate valent state. Here, it is found to be the most adequate description of TmSe, in accord with the intermediate valence nature of this compound.

As listed in Table II, the energy difference between the f^{13} and f^{12} configurations are -1.2, -13.5, -24.3, and -37.3 mRy, for TmS, TmSe, TmTe, and TmPo, respectively, reflecting again the trend towards greater localization with the larger ligand. The total energy of the f^{13} state is, however, found to be lower for all studied compounds, indicating that the SIC-LSD energy functional in fact overestimates the stability of this configuration, by an amount ~ 15 mRy. A similar overshooting was found for SmX compounds,[38] and most probably originates in the fact that the theory is still a one-electron theory, which does not take into account the energy gain due to multiplet formation in the f^{12} configuration (or f^5 configuration for Sm). A somewhat different approach, which replaces the atomic polarization energy of the SIC functional with experimental data, gives similar errors, but in this case with the trivalent phase too low in energy.[39]

The lattice constants obtained for the f^{12} configuration for TmTe and TmPo come close to the old values measured for TmTe[36] and TmPo,[35] corroborating the suggestion that these are in fact mixed valent samples. The TmS compound seems to be inappropriately described both by LSDA and SIC-LSD theory, since in both cases the f bands appear at the Fermi level, which should similarly be interpreted as an intermediate valent situation. Experimentally, TmS appears to be in a relatively pure trivalent ground state.[1] This is most distinctly supported by the photoemission spectra, which will be discussed in the next section. In the present f^{12} configuration the additional f band at the Fermi level is approximately 60% populated for both TmS and TmSe, leading to an average valency of ~ 2.4 for both, where the best estimate from experiment (lattice constant and photoemission) is 3 for TmS, 2.75 for TmSe, and 2 for TmTe,[1] or 2.91, 2.79, and 2.15 from resonant photoemission,[21] or 2.80, 2.53, and 2.02 from susceptibility.[21] Hence, in particular, the calculated valency of TmS is too low compared to these experimental estimates. The reason for the lower effective valencies calculated with the SIC-LSD approach is the too low position of the partly occupied f bands with respect to the Tm s-d band. The LDA+U method applied to TmS[18] is however capable of finding a ground state close to pure trivalent f^{12}, although the procedure of applying the U-shift in the band structure in this method is uncertain. The SIC-LSD approach in its present implementation mostly resembles that version of the LDA+U method where all of the U-shift is applied to the occupied states.

The calculated bulk moduli are presented in Table II where they are compared to available experimental data. The bulk moduli, $B(V)=V\partial^2E/\partial V^2$, are calculated from a 4th order polynomial fit of the total energies around the respective equilibrium volumes. Around the energy minimum they follow the expected trend, i.e., to decrease with increasing volume (by about 5–10 GPa per Å^3), except for TmTe in the f^{13} configuration (divalent) where the bulk modulus first decreases slightly with increasing pressure before increasing again. This qualitative behavior appears to be consistent with the experimental volume dependence of the bulk moduli for TmSe and TmTe.[42] The bulk moduli are very sensitive to the localization scenario which is due mainly to two factors: (i) the second derivative of the total energy with respect to volume depends on the degree of localization, and (ii) their volume dependence make them very sensitive to the actual equilibrium volume. In general, the stiffness is largest for the f^{12} configuration, the exception being once again TmTe where LSDA gives a somewhat higher value, whereas it is always smallest for the divalent f^{13} case. Another general trend from our calculations is that the softness of Tm monochalcogenides increases with the size of the ligand. It is not easy to find any systematics in the experimental bulk moduli reported in the literature (see Table II). It seems that, all compounds confounded, the experiments based on measuring the equation of state[8,9,41–44] report bulk moduli in the range 30–45 GPa whereas those based on ultrasonic measurements of the elastic constants[40,45,46] are around 80 GPa. Such a scattering of the experimental results makes it virtually impossible to draw any conclusion for the f-electron localization on that basis.

The comparison of the enthalpies, $H=E_{\mathrm{tot}}+PV$, for the different localization scenarios gives some insight into the pressure induced valence transitions of the Tm monochalcogenides. Figure 2 shows the calculated enthalpy differences between the f^{12} and the f^{13} cases for the different compounds. The critical pressures, P_c, for the $\mathrm{Tm}^{2+}-\mathrm{Tm}^{3+}$ transition can be obtained directly from our calculations when $\Delta H=0$ and are shown in Table II. These are all positive and are too large compared to the experiment. However, for reasons already discussed above in relation with equilibrium lattice constants, the stability of the f^{13} case is overestimated by the SIC-LSD method. When this fact is taken into account, i.e., when the f^{13} energies (or enthalpies) are shifted by the energy difference between the f^{12} and f^{13} states for TmSe (in order to make it a mixed valent at ambient pressure as is experimentally observed), the calculated critical pressure, P_c', are found to be in good agreement with experimental findings for TmTe[42] (2–5 GPa) and are predicted to be around -4 GPa for TmS and 8 GPa for TmPo (see Table II and Fig. 2).

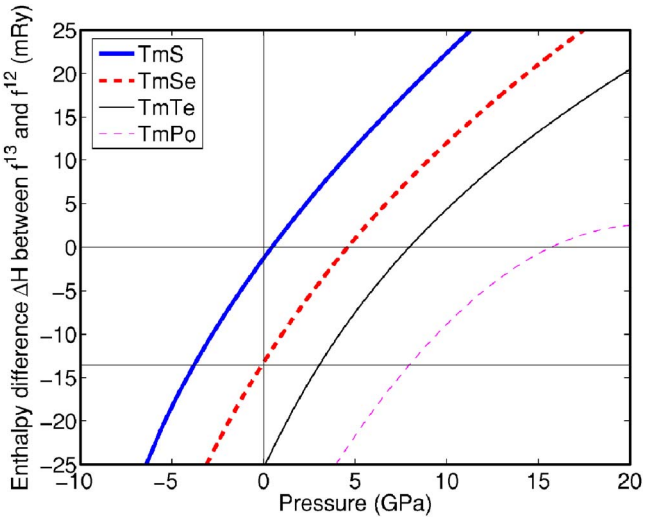

FIG. 2. (Color online) Enthalpy difference, ΔH, between the f^{12} and the f^{13} for the different Tm monochalcogenides. The critical pressures, P_c and P_c' in Table II can be read from the two lines at 0 and −13.5 mRy. This latter shift is just the energy difference between the f^{12} and f^{13} configurations for TmSe which is mixed valent at ambient pressure.

B. Photoemission spectra

In this section, the formalism outlined in Sec. II B is applied to compute the spectral functions of the TmX compounds. The experimental photoemission spectra[21,22] of these systems exhibit distinct multiplet features over a wide range of energies due to the localization of f electrons. This cannot be reproduced by the LDA, which only leads to a narrow f band at the Fermi level. In Figs. 3–5, the calculated spectral functions including multiplet effects of (respectively) TmS, TmSe, and TmTe are compared to available experimental data.[21–23]

For thullium sulfide, the experimental spectra are characterized by a broad band of f-related emission at large binding

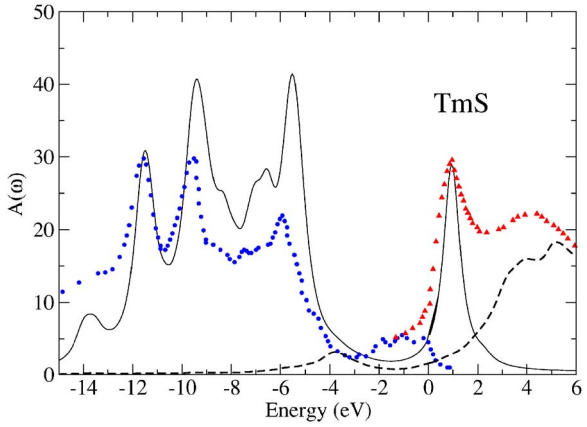

FIG. 3. (Color online) The calculated f contribution to the spectral function of TmS at equilibrium volume computed within the Hubbard-I method (full line) compared with x-ray photoemission spectroscopy (dots), and BIS (triangles) spectrum of Wachter *et al.*[23] The *spd* contribution from Tm to the total spectral function is shown as dashed lines. The Fermi level is put at zero energy.

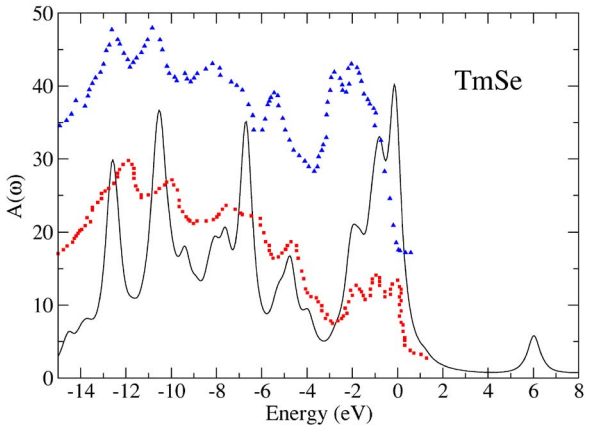

FIG. 4. (Color online) The calculated f-contribution to the spectral function of TmSe at equilibrium volume computed within the Hubbard-I method (full line) compared with the photoemission spectrum of Campagna *et al.*[22] (squares), and of Ufuktepe *et al.*[21] (triangles). The Fermi level is put at zero energy.

energies, in the range ∼−5 eV to ∼−14 eV, together with some features in the vicinity of the Fermi level. The deep emission features are related to $f^{12}\rightarrow f^{11}$ transitions, as also seen for the TmSb compound,[22] for which the three dominating peaks can be ascribed to the $f^{11}(^4I)$, $f^{11}(^4G)$, and $f^{11}(^2L)$ final states. Both the calculated and experimental spectrum reveal the three dominating peaks, at binding energies −5.6, −9.4, and −11.5 eV (theory), while experiment seems to find the first of these at slightly larger binding energy (around −6.0 eV). Even the shoulders at −8.3 eV [due to $f^{11}(^2H)$ final states] and around −7 eV [due to spin-orbit splitting of $f^{11}(^4I)$] are resolved, somewhat more clearly in the calculated spectra than in experiment. At lower binding energies only weak emission is observed, confirming the similarity of the ground state of the Tm ion in TmS to that in TmSb, i.e., a pure f^{12} configuration. For unoccupied states, a dominating $f^{12}\rightarrow f^{13}$ peak is found at 1.0 eV, in perfect agreement with the BIS (bremsstrahlung isochromat spectroscopy)

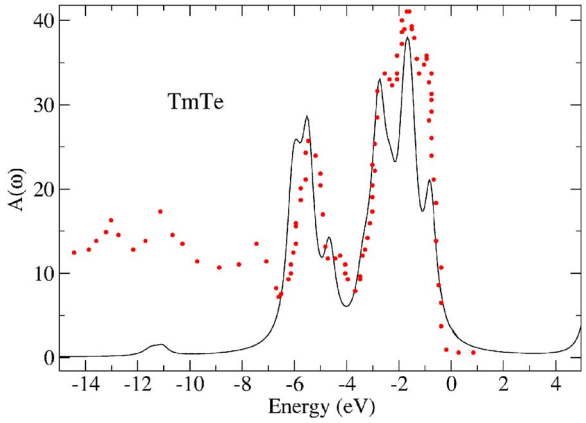

FIG. 5. (Color online) The calculated f contribution to the spectral function of TmTe at equilibrium volume computed within the Hubbard-I method (full line) compared with photoemission spectrum (dots) of Ufuktepe *et al.*[21] The Fermi level is put at zero energy.

experiment.[23] A second broad structure (around 4 eV) has been associated with Tm $5d$-$6s$ states[18] and is therefore not related to the multiplet of the f, shell. This is confirmed by the dashed line on Fig. 3 where we show the '*spd*' band contribution from Tm to the total spectral function. Notice that this contribution might also be responsible for the structures observed experimentally between 0 and −4 eV.

Thulium selenide is probably the most difficult case to handle due to its mixed valent character. Therefore, both the f^{12} and f^{13} configurations must be accounted for in the calculation. This requires a relatively sensitive tuning of the chemical potential of the reference atomic system such as to render the f^{12} and f^{13} nearly degenerate. The resulting spectrum is shown in Fig. 4. Clearly, this spectrum may be viewed as a superposition of the spectrum of TmTe (for binding energies between 0 and −6 eV) and that of TmS (from −6 to −15 eV). The characteristic three dominating peaks and shoulders of the $f^{12} \rightarrow f^{11}$ emission are distinct, now being calculated at ~1.2 eV larger binding energy compared to TmS. At low binding energies three narrow peaks, calculated at −0.2, −0.9, and −2.0 eV together with a broader feature at −4.8 eV, are signatures of the $f^{13} \rightarrow f^{12}$ emission with final states $f^{12}(^3H)$, $f^{12}(^3F)$, $f^{12}(^1G)$, and $f^{12}(^1I)$, respectively.[22] Note that Fig. 4 includes two experimental spectra[21,22] reported for TmSe, which seem to deviate somewhat with respect to the position of the Fermi level. Both reveal, however, the signatures of $f^{12} \rightarrow f^{11}$ as well as $f^{13} \rightarrow f^{12}$ emission, the present calculations being apparently in best agreement with the spectrum of Ref. 22. The relative weight of the $f^{12} \rightarrow f^{11}$ and $f^{13} \rightarrow f^{12}$ features in the experimental spectra are quite sensitive to matrix elements and resonance effects, while the theoretical calculations are sensitive to the Boltzmann weights [cf. Eq. (9)] of the two components of the ground state. A further uncertainty in the comparison of theory and experiment is concerned with possible surface effects. Notice that the spectral function of TmSe has already been calculated within the HIA approximation.[20] However, this calculation did not take into account the spin-orbit term [see Eq. (7)], and also used slightly different values of F^l.

The results for TmTe are presented in Fig. 5 together with the experimental results from Ref. 21. In this case, the chemical potential of the reference atom has been chosen so as to give a ground state of the thulium ion of f^{13}. Also in this case we find a good description of the experimental results by the present HIA theory. The three peaks located at binding energies of approximately −0.9, −1.6, and −2.7 eV are well placed in our calculation compared to experiment. Compared to the same features in TmSe, these peaks have moved towards larger binding energies by ~0.7 eV. The two additional structures, observed at −4.3 and −5.5 eV, appear as well in theory, but HIA gives them too low in energy by about 0.5 eV. The additional week structures observed at ~−8, −11, and −13 eV could indicate the presence of small amounts of f^{12} Tm ions, which are not reproduced by the present theory. As already discussed different samples of TmTe do show different degrees of trivalency, so it might be a question of sample and/or surface purity.

For the three compounds, the calculated Slater integrals have values close to F^0=31.9 eV, F^2=14.7 eV, F^4=9.1 eV, and F^6=6.5 eV. F^0 was rescaled to account for screening effects, to give a value of F^0=8 eV. Similarly, the computed spin-orbit constant ξ [see Eq. (7)] is largely independent of the ligand atom, with a value of approximately 0.34 eV. The invariance of these parameters shows that the effect of the environment of the thulium ion is weak on the $4f$ wave functions, but sufficient to induce a change in the valency.

Finally, it is worth noting that the spectrum of the TmX compounds has to some extent been reproduced by Antonov *et al.*[18] Their approach, which uses a weighted sum of LDA+U f density of states in order to mimic multiplet structures, is however, less well-defined than HIA from the theoretical point of view, and has probably limited predictive capability.

IV. SUMMARY

The electronic structures of Tm chalcogenides have been investigated. The total energy was calculated on the basis of the SIC-LSD approximation, and the ground states of TmTe and TmPo were best described in terms of a localized f^{13} Tm configuration, while TmS and TmSe are characterized by a localized f^{12} Tm configuration and a narrow and partly occupied f band pinned at the Fermi level. This situation is interpreted as the DFT realization of the mixed valent state, i.e., the best single-Slater determinant representing fluctuations between the f^{12} and f^{13} configurations.

The photoemission spectra of TmS, TmSe, and TmTe were calculated using the Hubbard-I approximation, in which an isolated reference ion of f^n configuration is exactly diagonalized and subsequently embedded in the solid state environment. The detailed multiplet structures of the experimental photoemission spectra were well described with an essentially pure f^{12} ground state of TmS, a mixed $f^{12}+f^{13}$ ground state of TmSe, and a pure f^{13} configuration of TmTe. The only inconsistency of the two approaches seems the overestimation of the mixed valent character of TmS in the SIC-LSD description.

ACKNOWLEDGMENTS

This work was partially funded by the EU Research Training Network "*Ab initio* Computation of Electronic Properties of f-electron Materials" (Contract No. HPRN-CT-2002-00295). Support from the Danish Center for Scientific Computing is also acknowledged. We also acknowledge support from the Swedish Research Council (V.R.) and the EU network EXCITING.

APPENDIX

Formally, the Hubbard-I approximation is a first-order perturbation theory in the hopping term in the Hamiltonian

$$H_t = \sum_{\substack{i \neq j \\ mm'}} t_{ij}^{mm'} c_{im}^{\dagger} c_{jm'}, \tag{A.1}$$

where m labels both orbital and spin indices. Considering the hopping term (A.1) as a small external potential one can

write a formally exact expression for the corresponding variation of the Green's function

$$\delta\hat{G} = \hat{G}\hat{\gamma}\hat{t}\hat{G}, \tag{A.2}$$

where $\hat{\gamma}$ is the three-leg vertex

$$\hat{\gamma} = 1 + \hat{\Gamma}\hat{G}\hat{G} \tag{A.3}$$

and $\hat{\Gamma}$ is the four-leg vertex.[47] One has to calculate $\hat{\gamma}$ in zeroth-order approximation in the hopping. Thus the Green's function $\hat{G}$ is diagonal in the site indices. Assuming that the Coulomb interaction matrix is also diagonal in the site indices [the Hubbard-type Hamiltonian; Eq. (7)] one can see that, due to the conservation of the site index at any interaction vertex there are no nontrivial diagrams contributing to δG_{ij} at $i \neq j$ and one has to replace $\hat{\gamma}$ by 1 in Eq. (A.2). This leads to the following equation: $\delta\hat{G}^{-1} = -\hat{t}$ and justifies the Hubbard-I approximation Eqs. (9) and (10), where we used the realistic hopping terms from the LDA Hamiltonian.

[1] P. Wachter, *Handbook on the Physics and Chemistry of Rare Earths* (Elsevier, Amsterdam, 1994), Vol. 19, Chap. 132, p. 177.
[2] E. Bucher, K. Andres, F. J. di Salvo, J. P. Maita, A. C. Gossard, A. S. Cooper, and G. W. Hull Jr., Phys. Rev. B **11**, 500 (1975).
[3] See articles in *Valence Fluctuations in Solids*, edited by L. M. Falikov, W. Hanke, and M. B. Maple (North-Holland, Amsterdam, 1981); and *Valence Instabilities*, edited by P. Wachter and H. Boppart (North-Holland, Amsterdam, 1982).
[4] J. M. Mignot and P. A. Alekseev, Physica B **215**, 99 (1995).
[5] K. Andres, W. M. Walsh, S. Darack, L. W. Rupp, and L. D. Longinotti, Solid State Commun. **27**, 825 (1978).
[6] A. Berger, E. Bucher, P. Haen, F. Holzberg, F. Lapierre, T. Penney, and R. Tournier, in *Valence Instabilities and Related Narrow Band Phenomena*, edited by R. D. Parks (Plenum, New York, 1977), p. 491.
[7] T. Matsumura, T. Kosaka, J. Tang, T. Matsumoto, H. Takahashi, N. Mori, and T. Suzuki, Phys. Rev. Lett. **78**, 1138 (1997).
[8] S. Heathman, T. L. Bihan, S. Darracq, C. Abraham, D. J. A. De Ridder, U. Benedict, K. Mattenberger, and O. Vogt, J. Alloys Compd. **230**, 89 (1995).
[9] J. Tang, T. Kosaka, T. Matsumara, T. Matsumoto, N. Mori, and T. Suzuki, Solid State Commun. **100**, 571 (1996).
[10] P. Link, I. N. Goncharenko, J. M. Mignot, T. Matsumura, and T. Suzuki, Phys. Rev. Lett. **80**, 173 (1998).
[11] J. Schoenes, J. Alloys Compd. **250**, 627 (1997).
[12] T. Matsumura, Y. Haga, Y. Nemoto, S. Nakamura, T. Goto, and T. Suzuki, Physica B **206**, 380 (1995).
[13] E. Clementyev, R. Köhler, M. Braden, J. M. Mignot, C. Vettier, T. Matsumura, and T. Suzuki, Physica B **230**, 735 (1997).
[14] P. Link, A. Gukasov, J. M. Mignot, T. Matsumura, and T. Suzuki, Phys. Rev. Lett. **80**, 4779 (1998).
[15] P. Wachter, F. Bommeli, and M. Filzmoser, Solid State Commun. **108**, 641 (1998).
[16] P. K. Jha, Solid State Commun. **126**, 159 (2003).
[17] H. J. F. Jansen, A. J. Freeman, and R. Monnier, J. Magn. Magn. Mater. **47–48**, 459 (1985).
[18] V. N. Antonov, B. N. Harmon, and A. N. Yaresko, Phys. Rev. B **63**, 205112 (2001).
[19] V. N. Antonov, B. N. Harmon, and A. N. Yaresko, Physica B **213–313**, 373 (2001).
[20] A. I. Lichtenstein and M. I. Katsnelson, Phys. Rev. B **57**, 6884 (1998).
[21] Y. Ufuktepe, S. Kimura, T. Kinoshita, K. G. Nath, H. Kumigashira, T. Takahashi, T. Matsumura, T. Suzuki, H. Ogasawara, and A. Kotani, J. Phys. Soc. Jpn. **67**, 2018 (1998).
[22] M. Campagna, E. Bucher, G. K. Wertheim, D. N. E. Buchanan, and L. D. Longinotti, Phys. Rev. Lett. **32**, 885 (1974).
[23] P. Wachter, S. Kamba, and M. Grioni, Physica B **252**, 178 (1998).
[24] A. Svane, W. M. Temmerman, Z. Szotek, J. Lægsgaard, and H. Winter, Int. J. Quantum Chem. **77**, 799 (2000).
[25] A. Svane and O. Gunnarsson, Phys. Rev. Lett. **65**, 1148 (1990).
[26] Z. Szotek, W. M. Temmerman, and H. Winter, Phys. Rev. B **47**, R4029 (1993).
[27] P. Hohenberg and W. Kohn, Phys. Rev. **136**, B864 (1964).
[28] W. Kohn and L. J. Sham, Phys. Rev. **140**, A1133 (1965).
[29] R. O. Jones and O. Gunnarsson, Rev. Mod. Phys. **61**, 689 (1989).
[30] J. P. Perdew and A. Zunger, Phys. Rev. B **23**, 5048 (1981).
[31] J. Hubbard, Proc. R. Soc. London **276**, 238–257 (1963); **277**, 237–259 (1964); **281**, 401–419 (1964).
[32] V. I. Anisimov, F. Aryasetiawan, and A. I. Lichtenstein, J. Phys.: Condens. Matter **9**, 767 (1997).
[33] V. I. Anisimov, A. I. Poteryaev, M. A. Korotin, A. O. Anokhin, and G. Kotliar, J. Phys.: Condens. Matter **9**, 7359 (1997).
[34] F. de Groot, Coord. Chem. Rev. **249**, 31 (2005).
[35] C. J. Kershner, R. J. DeSando, R. F. Heidelberg, and R. H. Steinmeyer, J. Inorg. Nucl. Chem. **28**, 1581 (1964).
[36] A. Iandelli, Rend. Accad. Naz. Lincei **37**, 160 (1964).
[37] P. Villars and L. D. Calvert, *Pearson's Handbook of Crystallographic Data for Intermetallic Phases* (ASM International, Metals Park Ohio, 1991), 2nd ed.
[38] A. Svane, V. Kanchana, G. Vaitheeswaran, G. Santi, W. M. Temmerman, Z. Szotek, P. Strange, and L. Petit, Phys. Rev. B **71**, 045119 (2005).
[39] A. Delin, L. Fast, B. Johansson, J. M. Wills, and O. Eriksson, Phys. Rev. Lett. **79**, 4637 (1999).
[40] Y. Nakanishi, S. Takuo, M. Motokawa, T. Matsumura, Y. Nemoto, H. Hazama, T. Goto, and T. Suzuki, Phys. Rev. B **64**, 184434 (2001).
[41] H. Boppart, A. Treindl, P. Wachter, and S. Roth, Solid State Commun. **35**, 483 (1980).
[42] D. Debray, A. Werner, D. L. Decker, M. Loewenhaupt, and E. Holland-Moritz, Phys. Rev. B **25**, 3841 (1982).
[43] H. Boppart, J. Magn. Magn. Mater. **47–48**, 436 (1985).
[44] A. Jayaraman, A. K. Singh, A. Chatterjee, and S. Usha Devi, Phys. Rev. B **9**, 2513 (1974).
[45] T. Matsumura, S. Nakamura, T. Goto, H. Amitsuka, K. Matsuhira, T. Sakakibara, and T. Suzuki, J. Phys. Soc. Jpn. **67**, 612 (1998).
[46] Y. Nakanishi, T. Sakon, T. Matsumura, Y. Nemoto, H. Hazama, T. Goto, T. Suzuki, and M. Motokawa, J. Magn. Magn. Mater. **226–230**, 164 (2001).
[47] A. B. Migdal, *Theory of Finite Fermi Systems and Applications to Atomic Nuclei* (Wiley, New York, 1967).